Letter | Editors' Suggestion

Magnetoionic control of perpendicular exchange bias

J. Zehner,[1,2,3] D. Wolf,[1] M. U. Hasan,[4] M. Huang,[4] D. Bono,[4] K. Nielsch,[1,2] K. Leistner,[1,3] and G. S. D. Beach[4]

[1]*Leibniz IFW Dresden Helmholtzstrasse 20, Dresden 01069, Germany*

[2]*Institute of Material Science TU Dresden, Dresden 01062, Germany*

[3]*Faculty of Natural Sciences, Institute of Chemistry, Chemnitz University of Technology, Straße der Nationen 62, 09111 Chemnitz, Germany*

[4]*Department of Materials Science and Engineering, Massachusetts Institute of Technology, Cambridge, Massachusetts 02139, USA*

(Received 19 April 2021; accepted 2 June 2021; published 21 June 2021)

We demonstrate reversible voltage control of perpendicular exchange bias via H^+ pumping in a NiO/Pd/Co/Pd/$Gd(OH)_3$/Au heterostructure at room temperature. The perpendicular exchange bias results from a tailored layer structure consisting of an antiferromagnetic NiO layer and a ferromagnetic Co layer, stabilized by an ultrathin Pd interlayer. Voltage mediated H^+ pumping through the $Gd(OH)_3$ layer and subsequent H absorption at the Pd/Co interface leads to a decrease in the perpendicular anisotropy. In consequence, also the perpendicular exchange bias vanishes upon voltage application (3V). During voltage switch-off, this process reverses and perpendicular exchange bias recovers. The first voltage switching cycle shows relatively slow kinetics and an inverse relation of exchange bias and coercivity changes. We discuss these features with regard to an H-induced crystallization of the initially amorphous Pd/Co/Pd trilayer, which is revealed by transmission electron microscopy. With subsequent voltage switching steps, a decrease of the exchange bias field in the voltage switch-off state is observed, which levels off with increasing cycle numbers. A reversible setting of exchange bias field values is achieved when a magnetic field (+/− 2 kOe) is superposed during the H loading step. In this case, the shift of the exchange bias field can be controlled by the direction of the applied magnetic field. These results open an innovative route to electrically control exchange bias.

DOI: 10.1103/PhysRevMaterials.5.L061401

I. INTRODUCTION

In modern nanomagnetic based technology, exchange bias (EB) is required for giant- or tunneling magnetoresistive sensors [1–3]. Research on EB has started in 1956 [4] and the EB systems under investigation showed a magnetization in the film plane. The first report on perpendicular EB was published in 2001 [5]. Since then, perpendicular EB is highly interesting for fundamental and applied research, [6] mainly due to the advantages of a low susceptibility to thermal noise [7], and a fast switching speed [8–10].

EB is observed in heterostructures where a ferromagnet (FM) and an antiferromagnet (AFM) share an interface [2–4]. The interfacial exchange coupling between the FM and AFM results macroscopically in a shift of the hysteresis loop along the magnetic field axis [11,12]. EB can be set thermally [13–15] or spontaneously via a structural phase transition in the AFM [16].

Voltage control of ferromagnetic metals has evolved in recent years as a promising approach towards low-power switching of magnetic properties. [17–22] Voltage control of the EB was already demonstrated by utilizing common magnetoelectric systems (e.g., multiferroics). [23–27] These systems often show the disadvantage of complex epitaxial layer deposition procedures, operation below room temperature or the requirement for large voltages (kV to MV) to achieve changes in EB. In contrast, voltage-control of magnetism by ion migration benefits from relatively simple demands on the sample quality (e.g., polycrystalline films) and low voltage requirements (few volts). With ionic mechanisms, large, reversible and nonvolatile tuning of, e.g., H_C or M_S has been demonstrated at room temperature, which opens a route towards ultralow power magnetic memory/storage, stochastic- and neuromorphic computing and the design of energy efficient nanodevices in general. [17,19,20,28–35] Such effects are currently summarized under the generic term "magnetoionic control". So far, research on magnetoionic effects in thin films focused on the control of the properties of a magnetic layer sandwiched between an underlying (electron-) conducting layer and an electrolyte as the ion reservoir. [22,36–40] Only few reports exist on changing the EB by magnetoionic control [41–46]. In IrMn/Fe/FeO_x films gated via an alkaline electrolyte, voltage-induced modulation of the in-plane EB was achieved via redox reactions in the ferromagnetic layer at room temperature. [43] For perpendicular EB systems, only one publication [46] reports on magnetoionic effects on the H_C and the H_{EB}. Oxygen ion migration is utilized to achieve a change of ≈60% in H_C and up to ≈80% in H_{EB}. However, these oxygen-ion induced changes of the magnetic properties were rather slow (gated by ionic liquid for 30 min at room temperature) and measured at very low temperatures (10 K).

Recently, the transfer from oxygen ion to hydrogen ion-based mechanisms has led to a significant improvement in reversibility and switching speed of magnetoionic effects in all-solid-state devices. [29] By pumping hydrogen ions

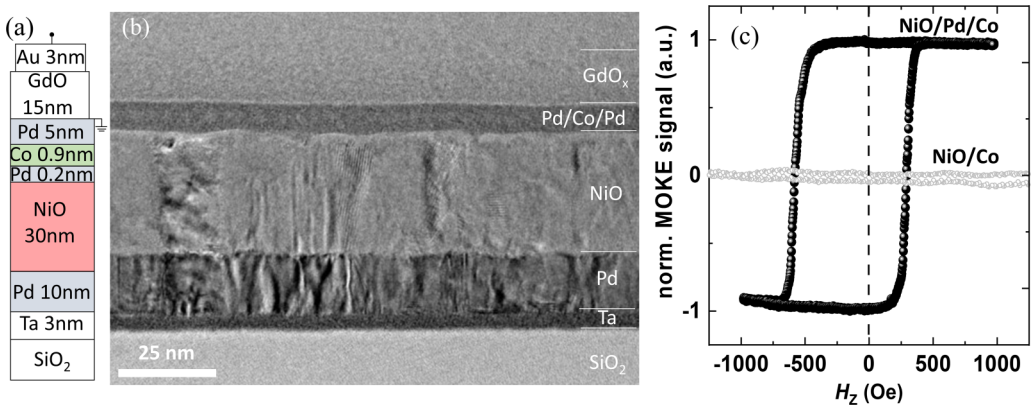

FIG. 1. (a) Schematic illustration of the sputter deposited layer architecture and electrode connections for H^+ pumping experiments. (b) Cross-section BFTEM image of the layer stack. (c) Magnetization curves for layer stacks with (black symbols) and without (grey symbols) a 0.2 nm Pd interlayer between the NiO and Co layers as measured by polar MOKE magnetometry.

through a hydrated rare-earth oxide layer, fast (ms regime) and highly reversible (>1000 cycles) toggling between in-plane and perpendicular magnetic anisotropy was achieved in Co/Pd thin films. [29,47,48] This effect relies on the voltage-induced pumping of H into the Pd layer, which leads to a change of interface magnetic anisotropy of the adjacent Co layer. [49] We extend this concept to the magnetoionic control of thin films with perpendicular EB. Details on the sample preparation and measurements are in the Appendices.

II. RESULTS

The layer stack, depicted in Fig. 1(a), is designed for voltage control of perpendicular EB by hydrogen pumping. The transmission electron microscopy (TEM) cross-sectional image in Fig. 1(b) shows the layer architecture in the as-deposited state. The Ta/Pd double layer is used as a buffer layer for adhesion and the Pd/$Gd(OH)_3$ layers function as the material for the hydrogen pumping [29]. The ultrathin Co layer (0.9 nm) serves as the ferromagnetic layer with perpendicular magnetic anisotropy, and the NiO layer (30 nm) serves as the antiferromagnetic layer. Between the NiO layer and the Co layer, an ultrathin Pd interlayer (0.2 nm) is inserted, which is found decisive for the achieving the perpendicular EB. Without this Pd interlayer, i.e., when the Co layer is in direct contact with the NiO layer, neither an out-of-plane [Fig. 1(c) grey line], nor an in-plane (not shown) magnetization curve is detected by magneto-optical Kerr effect (MOKE) magnetometry. As a result, the optimized layer stack (SiO_2/Ta/Pd/NiO/Pd/Co/Pd/GdO/Au) exhibits the desired magnetization curve displaying perpendicular exchange bias [Fig. 1(c) black curve]. The loop shift along the magnetic field axis is opposite to the direction of the external magnetic field applied during deposition. Such a negative EB is commonly found in most EB systems. [1]

For voltage tuning of the perpendicular exchange bias field (H_{EB}), we investigate the influence of H loading [29] on the magnetic properties of the EB layer stack. Figure 2 illustrates the influence of an applied voltage on the perpendicular magnetization curves. Figure 2(a) shows the curve of the virgin state (after hydration of the GdO_x layer). In order to induce the hydrogen switching mechanism [29], we apply a gate voltage (V_G) of $V_G = +3$ V to trigger the water-splitting reaction and induce H absorption in the Pd/Co/Pd layers. [29,47] At $V_G = +3$ V is applied, a continuous change in the magnetization curves occurs, which reflects a decrease in the perpendicular anisotropy [Figs. 2(b)–2(d)]. After 138 s at +3 V [Fig. 2(d)], the closed magnetization curve with vanishing M_R/M_{1000Oe} ratio and coercivity (H_C) reveals a fully in-plane anisotropy state. When the applied voltage is set back to 0 V, the hysteresis loop recovers to an out-of-plane state [Figs. 2(e)–2(g)]. With this transition from the out-of-plane to the in-plane state and vice versa, the perpendicular exchange bias vanishes and recovers. The absolute value of the exchange bias field of the recovered state [$|H_{EB}| = 83$ Oe in Fig. 2(g)] is decreased compared to the virgin state [$|H_{EB}| = 151$ Oe in Fig. 2(a)]. In contrast, the coercivity of the recovered loop [$H_C = 425$ Oe in Fig. 2(a)] is larger than that of the virgin loop [$H_C = 522$ Oe in Fig. 2(g)].

In order to study the influence of multiple H^+ pumping steps on the observed magnetoionic control of EB, the magnetic properties were measured during 11 switching cycles with repeated application of $V_G = +3$ V and $V_G = 0$ V (Fig. 3). To exclude that the effects are related to the consecutive cycling of the magnetic field, the hysteresis loop of the same sample was continuously measured for about 250 s before the voltage was applied for the first time. In this case, no change in magnetic properties (not shown) and exchange bias [grey data points in Fig. 3(c)] occurred. The changes of the M_R/M_{1000Oe} ratio, coercivity and exchange bias field for the repeated voltage application are shown in Figs. 3(a), 3(b), and 3(c), respectively. The grey shaded areas in Fig. 3 mark the times when $V_G = +3$ V is applied and the white areas mark the times when $V_G = 0$ V. At $V_G = 0$ V, a large M_R/M_{1000Oe} ratio [Fig. 3(a)] and a large H_C [(Fig. 3(b)] are always present, which are connected to the state with perpendicular anisotropy. The repeatable switching to the in-plane state (reflected in the vanishing M_R/M_{1000Oe} ratio and decrease of H_C) is achieved for all voltage gating steps ($V_G = +3$ V), proving the reversibility of the magnetoionic control. An appreciable perpendicular exchange bias only occurs for the states with perpendicular anisotropy at $V_G = 0$ V [therefore, the H_{EB} values are plotted exclusively for these steps in Fig. 3(c)]. Thus, with the results in Fig. 3, we demonstrate

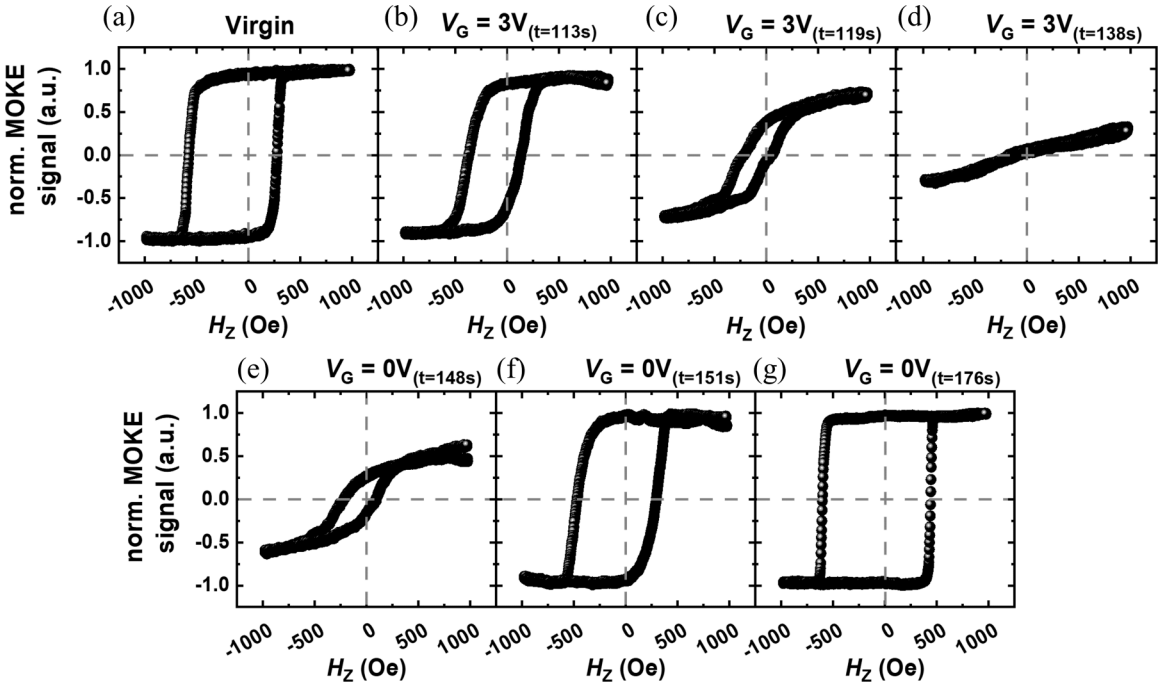

FIG. 2. Voltage dependent perpendicular magnetization curves of an EB layer stack upon H^+-pumping. (a) Virgin state. (b)–(d) states at $V_G = +3$ V, showing the decreasing perpendicular anisotropy over time (t), and (e)–(g) at $V_G = 0$ V showing the recovery of perpendicular anisotropy and exchange bias over time.

a reversible voltage-controlled ON/OFF-switching of perpendicular EB via ionic migration.

Besides the reversible switching between the in-plane and out-of-plane states, Fig. 3 shows some distinct features for the first switching cycle. After the first voltage application, in accordance with the results in Fig. 2, a decreased (negative) exchange bias field and an increased coercivity is observed in the recovered state (0 V), in comparison to the virgin state. In the subsequent cycles, only a moderate further decrease in $-H_{EB}$ and marginal increase in H_C are measured for the recovered states (0 V). Further, the time required for the switching to the in-plane state at $V_G = +3$ V becomes significantly shorter after the first cycle.

For a control of the EB in the recovered states during several switching cycles, we investigate the influence of a superposed (out-of-plane) magnetic field during H^+ pumping. The application of a constant magnetic field was already shown to increase/decrease the exchange bias field of a virgin sample by about 5% (see Fig. S1 in the Supplemental Material [50]). Figure 4 shows the influence of a superimposed magnetic field of +/− 2 kOe at $V_G = +3$ V on the exchange bias field measured afterwards for the recovered state (0 V).

The open black data point in Fig. 4 corresponds to the last measurement step in Fig. 3(c). Then, a positive magnetic field of +2 kOe and simultaneously $V_G = +3$ V were applied for 10 s. After setting the voltage back to 0 V, the recorded hysteresis loop shows an increase in $-H_{EB}$ by about 10%. The measurements sequence was repeated, but with the superposition of a negative magnetic field of −2 kOe. In this case, after voltage switch -off, a decrease of $-H_{EB}$ by about 15% is obtained with respect to the starting state (open black data point in Fig. 4). This measurement procedure was repeated three times and resulted in a similar increase/decrease of the exchange bias field for positive/negative applied magnetic fields.

In order to understand the magnetoionic mechanism in more detail, the cross-section of the EB layer stack was characterized by high resolution (HR)-TEM before and after the H^+ pumping procedure (Fig. 5). In the virgin state [Fig. 5(a)], an amorphous Pd/Co/Pd layer is observed on top of the crystalline NiO layer. In contrast, after the H^+ pumping (after cycle $n = 8$ in Fig. 4), a crystalline structure is observed for the Pd/Co/Pd layer, with epitaxial alignment to the NiO layer. In addition, crystallized areas are also visible within the $Gd(OH)_3$ layer after H^+ pumping.

III. DISCUSSION

We achieve voltage control of perpendicular exchange bias by applying hydrogen-based magnetoionics to a tailored layer stack. For this, we introduced an antiferromagnetic NiO underlayer in a $Co/Pd/Gd(OH)_3$ heterostructure, in which the Co layer is known to be susceptible to hydrogen-based magnetoionic control. [29]

We found that the ultrathin Pd interlayer (0.2 nm) on top of the NiO layer, prior to Co deposition, is crucial for EB. Our results indicate that the direct deposition of Co on the NiO layer leads to the formation of nonferromagnetic CoO_x. The introduction of the ultrathin Pd interlayer most likely avoids this oxidation process and leads to the stabilization of the ferromagnetic Co. Interestingly, the Pd interlayer does not impede the interfacial coupling between the antiferromagnetic NiO and the ferromagnetic layer. However, this agrees with a study on ferromagnetic Co/Pt multilayers which also display perpendicular EB despite the presence of an ultrathin Pt spacer layer between the FM and the AFM FeMn layer. [51] We

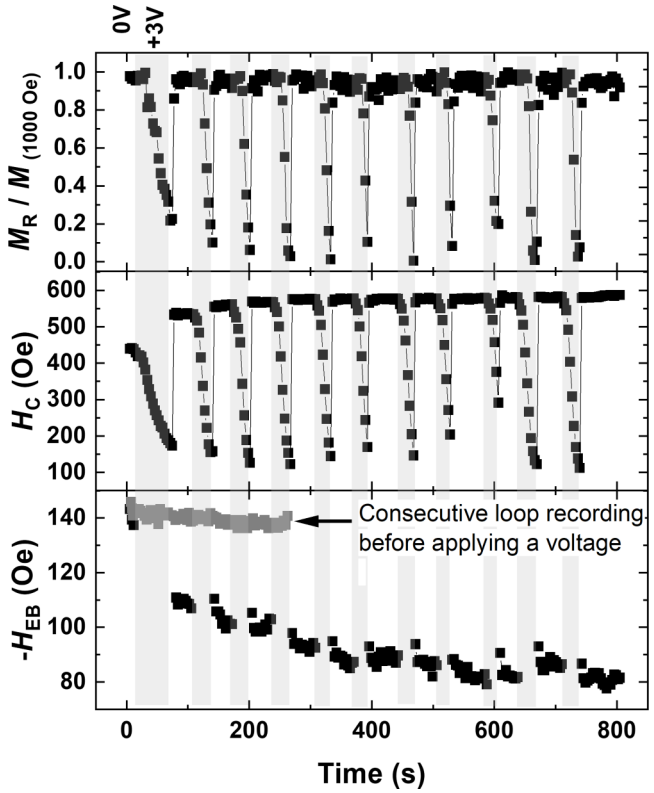

FIG. 3. (a) $M_R/M_{1000\text{Oe}}$ ratio, (b) H_C and (c) H_{EB} extracted from out-of-plane MOKE hysteresis measurements versus time as V_G is repeatedly set between +3 V (grey shaded area) and 0 V.

propose that the stabilization of EB could be connected to the formation of a Co-Pd alloy at the interface. This is consistent with the HR-TEM images of the virgin state [Fig. 5(a)] and the elemental mapping after H^+ pumping [Fig. 5(c)], in both of which the ultrathin Pd interlayer is not clearly distinguishable as a separating layer between the Co and the NiO.

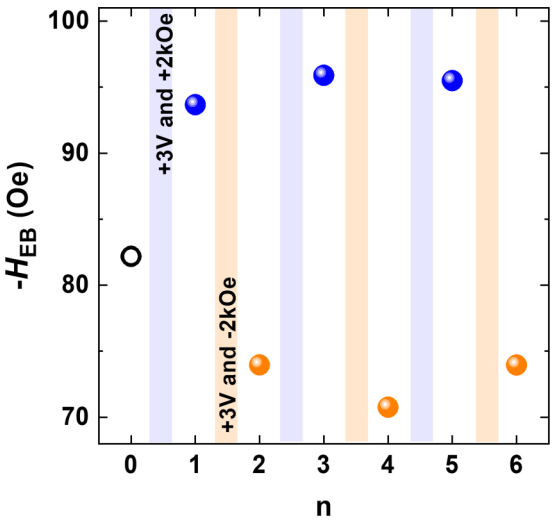

FIG. 4. Influence of a superimposed magnetic field during H^+ pumping on the exchange bias field of the recovered state afterwards (n is the measurement steps).

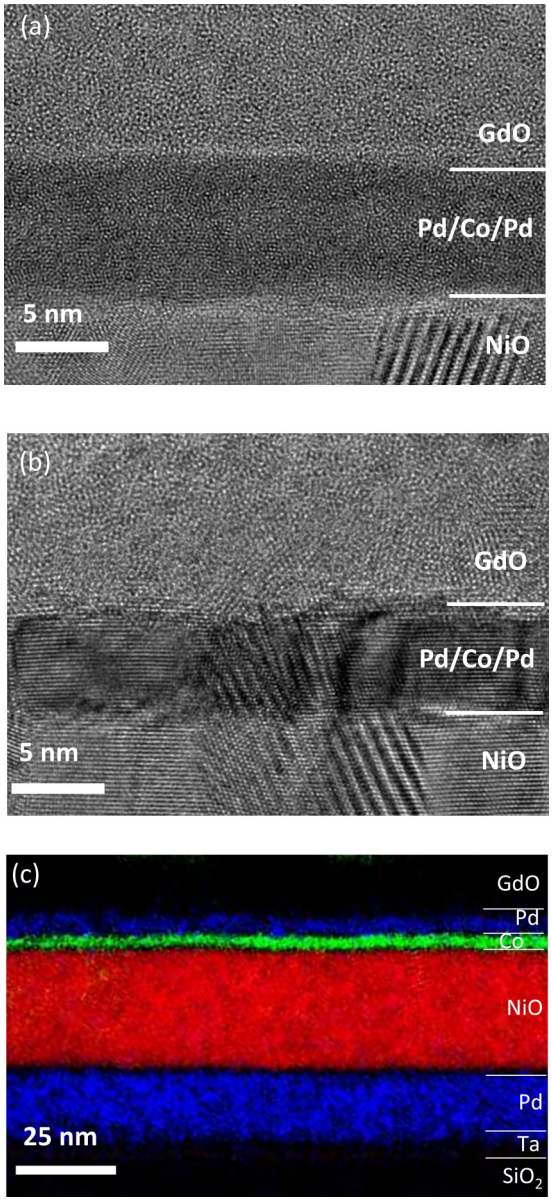

FIG. 5. Cross-sectional HR-TEM on an exchange bias layer stack. (a) Virgin sample and (b) sample after H^+ pumping. (c) Cross-section elemental mapping of a larger section of the film after H^+ pumping, where Pd, Ni and Co are color-coded in blue, red, and green, respectively.

Upon H^+ pumping, a decrease of coercivity and remanence ratio occurs and the perpendicular exchange bias vanishes. This behavior is reversible and can be directly explained by the decrease of perpendicular anisotropy of the Co layer due to voltage induced H^+ migration through the $Gd(OH)_3$ and subsequent H adsorption at the Co layer. [29] Thus, this presents the control of perpendicular EB via voltage induced hydrogen ion migration Our approach benefits from the application of a low voltage (3 V) compared to other magnetoelectric systems (kV to MV). [23–27] Improvements with regard to the switching speed can be achieved by selecting an optimized oxide [48]. We assume that also a careful investigation of the magnitude of the gate voltage could lead to faster switching.

Our system could thus provide further directions towards low power tunable perpendicular EB systems in high-density spintronic devices.

It is worth mentioning that the observed voltage induced H^+ pumping effects on the magnetic properties are localized within the area beneath the Au electrode. The magnetization curve characteristics next to the Au electrode are not affected, see Supplemental Material S2. In common voltage-induced EB control in multiferroic heterostructures, the EB is usually manipulated across the whole film area via strain coupling. [52] Only few reports are available which demonstrate a local patterning of EB via a voltage through resistive switching of the AFM layer [44] or a redox reaction of the FM layer [43]. Our results thus present an original approach for a local patterning of EB via a voltage. As here, no sophisticated vacuum systems are needed and just a simple electrode contacting set up is required, our approach would offer advantages over previously reported local EB patterning approaches via, e.g., laser or ion irradiation [53,54], on lithographically produced magnetic nanostructures [3,55] or on thermally assisted magnetic scanning probe lithography [56]. We thus propose voltage induced local patterning by H^+ pumping as another possibility for postfabrication control of EB systems.

The distinct differences in the first-time switching process (Fig. 3, 15–80 s) allow us to discuss the initial processes during magnetoionic switching. During the first-time gating at +3 V, a slower kinetics until the full in-plane switching is observed. Also, the changes in H_C and H_{EB} between virgin and recovered (0 V) state are larger after the first gating step than after the subsequent gating steps. Interestingly, a decrease in the negative exchange bias field (by $\approx -33\%$) is observed, while at the same time coercivity increases ($\approx +22\%$). This inverse scaling of H_C and $|H_{EB}|$ after the first H^+ pumping step is unusual. In common EB systems, H_C and $|H_{EB}|$ scale with each other, because the exchange bias gives an intrinsic contribution to coercivity. [57] Thus, in the present case, the coercivity increase cannot be caused by the change of the exchange bias, but must have a separate origin. Our results indicate that the distinct feature of the first cycle, namely the slow kinetics and the increase of coercivity, are related to a microstructural activation/transformation process. Upon H^+ pumping, hydration of the Pd layer is known to occur [29], which will lead to expansion and straining of the initial Pd layer. This could induce magnetoelastic effects in the Co layer and thereby impact coercivity. However, in the initial state, the Pd/Co/Pd structure is amorphous [Fig. 5(a)] and the magnetoelastic interactions are expected to be small due to the microstructural randomness. [58–61] In contrast, the observed transformation from amorphous to crystalline state in the Pd/Co/Pd layer region [Figs. 5(a) and 5(b)] provides a direct explanation for the increase in coercivity. We propose that crystallization is triggered when H enters the structure for the first time. Such H-induced crystallization of amorphous metals has indeed been reported previously. [62,63] Amorphous layers in general show softer magnetic properties (i.e., lower H_C) compared to their crystalline counterparts. [64,65] This can be understood by the introduction of grain boundaries in crystalline layers which add domain wall pinning sites to the system, and thereby lead to a coercivity increase. Thus, the increased coercivity after the first H^+ pumping step can be assigned to the introduction of grain boundaries upon crystallization. We propose that the solid-state crystallization process only occurs during the first-time hydrogenation. This is consistent with the prolonged switching time required during the first step. Also, the marginal change in H_C during the subsequent cycles [see Fig. 3(b)] indicates that crystallization is completed after the first cycle.

As a trend, the $|H_{EB}|$ of the recovered states (0 V) decreases with increasing cycle numbers. The rate of this decrease slows down and almost settles after cycle number 8 ($\sim$500 s in Fig. 3(c)]. This behavior could be due to a voltage-induced training effect [66] or/and a voltage-induced thermal after effect (see discussion S3 in the Supplemental Material). We demonstrated that this continuous decrease can be stopped by magnetic-field-assisted gating. Then, the polarity of the superposed magnetic field determines the direction of the EB change (Fig. 4). This possibility to tune the EB by superposing a gate voltage and a magnetic field provides an innovative route to design EB systems in general, e.g., as an alternative to field cooling procedures via postannealing treatments. Such magnetic-field assisted gating to control EB can be applied on a local scale and can be much faster than conventional methods for EB setting.

IV. CONCLUSION

We prepared NiO/Pd/Co/Pd-based thin films with perpendicular exchange bias suitable for magnetoionic control by H^+-pumping. The introduction of an ultrathin Pd interlayer proved decisive to establish the exchange bias in this layer system. Upon magnetoionic H^+ pumping achieved by voltage gating, the perpendicular magnetic anisotropy switches to in-plane magnetic anisotropy. In consequence, the associated remanence, coercivity, and exchange bias field of the ferromagnetic layer vanish during voltage-gating. The process reverses during voltage switch-off. We demonstrate that this low-voltage-induced switching of magnetic properties in a perpendicular EB system is highly reversible. For the first cycle, the magnetoionic process is slower and an increased coercivity is observed for the recovered state in comparison to the virgin state. These features are explained by a hydrogen-induced crystallization process of the initially amorphous Pd/Co/Pd layers. The absolute exchange bias field continuously decreases with the voltage cycling steps, indicating a voltage induced training effect and/or thermal after effect. We find that a combined voltage- and magnetic field routine is effective to increase and decrease the value of H_{EB} in a controlled manner. This work shows an innovative path towards local (voltage) control of exchange bias systems as well as magnetic nanodevices in general.

ACKNOWLEDGMENTS

The authors acknowledge funding by the Deutsche Forschungsgemeinschaft (DFG) (Project No. 400178764) and the excellence program initiative of the IFW Dresden. The authors thank T. Walter and A. Pöhl for TEM sample preparation.

APPENDIX A: SAMPLE PREPARATION

The layer system consisted of Ta (3 nm)/Pd (10 nm)/NiO (30 nm)/Pd (0.2 nm)/Co (0.9 nm)/Pd (5 nm)/GdO_x (10 nm)/Au (3 nm) layers grown on a thermally oxidized Si/SiO_2 substrate. For deposition, the substrate was mounted on a $1 \times 1\,cm^2$ surface of a flat permanent magnet, where a magnetic field of 2.8 kOe with the magnetic north pole perpendicular to the substrate surface existed. The layers were subsequently deposited by dc magnetron sputtering at room temperature and at 3 mTorr Ar pressure. The oxide layers were deposited via dc reactive sputtering with a partial oxygen pressure of 0.07 mTorr. Prior to GdOx deposition, a corner of the Pd/Co/Pd layer was protected with aluminum foil; this uncovered Pd/Co/Pd corner then served as the bottom contact for the gating experiments. After the layer deposition, the hydration of the GdO_x into $Gd(OH)_3$ was performed at 70 °C, following the procedure described in Ref. [47]. On top of the hydrated layer system, circular Au top electrodes with a diameter of 200 μm and a thickness of about 8 nm were fabricated using dc magnetron sputtering through a shadow mask.

APPENDIX B: MAGNETIC MEASUREMENTS

A polar MOKE setup was used for measuring the magnetization curves before and during the H^+ pumping experiments. The setup consisted of a 2.5-mW laser with a wavelength of 660 nm. The gate voltage was applied using one CuBe probe in contact with the edge of the circular Au top electrode and another CuBe probe in contact with the previously covered Ta/Pd/NiO/Pd/Co/Pd layer [see Fig. 1(a)]. All experiments were performed at room temperature. The ratio of the remanence (M_R) versus the magnetization at 1000 Oe (M_{1000Oe}) for the out-of-plane magnetization curve was determined by taking the MOKE intensity value at $H = 0$ in the ascending field branch of the normalized MOKE hysteresis loop.

APPENDIX C: STRUCTURE AND MICROSTRUCTURE MEASUREMENTS

TEM cross-section lift-out lamellas of the layer stack were prepared by focused ion beam milling. To resolve the nanoscopic structure of the layers, bright-field (BF) TEM and HRTEM were performed with an aberration-corrected Titan^3 80–300 TEM instrument (ThermoFisher Company, USA) providing a resolution of 0.08 nm. The TEM images were acquired at an acceleration voltage of 300 kV and recorded with a 2k by 2k slow-scan CCD camera (Type Gatan UltraScan1000). To conduct qualitative elemental mapping, we carried out energy-filtered TEM (three window method) using a postcolumn Gatan imaging filter (GIF Trideiem, Gatan, Inc., US). We thereby exploited the inner-shell electrons excitations of respective elements by the highly energetic TEM beam electrons. For Pd mapping we used the $M_{4,5}$ edge at 335 eV, for Co mapping the $M_{2,3}$ edge at 60 eV, and for Ni mapping the $M_{2,3}$ edge at 68 eV.

[1] J. Nogués and I. K. Schuller, Exchange bias, J. Magn. Magn. Mater. **192**, 203 (1999).

[2] A. E. Berkowitz and K. Takano, Exchange anisotropy—a review, J. Magn. Magn. Mater. **200**, 552 (1999).

[3] J. Nogués, J. Sort, V. Langlais, V. Skumryev, S. Suriñach, J. S. Muñoz, and M. D. Baró, Exchange bias in nanostructures, Phys. Rep. **422**, 65 (2005).

[4] W. H. Meiklejohn and C. P. Bean, New magnetic anisotropy, Phys. Rev. **102**, 1413 (1956).

[5] S. Maat, K. Takano, S. S. P. Parkin, and E. E. Fullerton, Perpendicular Exchange Bias of Co /Pt Multilayers, Phys. Rev. Lett. **87**, 087202 (2001).

[6] W. Zhang and K. M. Krishnan, Epitaxial exchange-bias systems: From fundamentals to future spin-orbitronics, Mater. Sci. Eng. R. Rep. **105**, 1 (2016).

[7] G. Kim, Y. Khaydukov, M. Bluschke, Y. E. Suyolcu, G. Christiani, K. Son, C. Dietl, T. Keller, E. Weschke, P. A. van Aken, G. Logvenov, and B. Keimer, Tunable perpendicular exchange bias in oxide heterostructures, Phys. Rev. Mater. **3**, 084420 (2019).

[8] A. D. Lamirand, M. M. Soares, A. Y. Ramos, H. C. N. Tolentino, M. De Santis, J. C. Cezar, A. de Siervo, and M. Jamet, Robust perpendicular exchange coupling in an ultrathin CoO/PtFe double layer: strain and spin orientation, Phys. Rev. B **88**, 140401(R) (2013).

[9] Y. Shiratsuchi, H. Noutomi, H. Oikawa, T. Nakamura, M. Suzuki, T. Fujita, K. Arakawa, Y. Takechi, H. Mori, T. Kinoshita, M. Yamamoto, and R. Nakatani, Detection and *In Situ* Switching of Unreversed Interfacial Antiferromagnetic Spins in a Perpendicular-Exchange-Biased System, Phys. Rev. Lett. **109**, 077202 (2012).

[10] S. Mangin, D. Ravelosona, J. A. Katine, M. J. Carey, B. D. Terris, and E. E. Fullerton, Current-Induced magnetization reversal in nanopillars with perpendicular anisotropy, Nat. Mater. **5**, 210 (2006).

[11] C. Chappert, A. Fert, and F. N. Van Dau, The emergence of spin electronics in data storage, Nat. Mater. **6**, 813 (2007).

[12] K. Elphick, K. O'Grady, and G. Vallejo-Fernandez, Perpendicular Exchange Bias in $(Co/Pt)_n$ Multilayers, IEEE Trans. Magn. **55**, 1 (2019).

[13] P. A. A. van der Heijden, T. F. M. M. Maas, W. J. M. de Jonge, J. C. S. Kools, F. Roozeboom, and P. J. van der Zaag, Thermally assisted reversal of exchange biasing in NiO and FeMn based systems, Appl. Phys. Lett. **72**, 492 (1998).

[14] A. Paetzold and K. Röll, Thermally activated self-alignment of exchange coupling in NiO/NiFe bilayers, J. Appl. Phys. **91**, 7748 (2002).

[15] L. Thomas and B. Negulescu, Metastable antiferromagnetic domain configurations in exchange biased bilayers, J. Appl. Phys. **93**, 8606 (2003).

[16] A. Migliorini, B. Kuerbanjiang, T. Huminiuc, D. Kepaptsoglou, M. Muñoz, J. L. F. Cuñado, J. Camarero, C. Aroca, G. Vallejo-Fernández, V. K. Lazarov, and J. L. Prieto, Spontaneous exchange bias formation driven by a structural phase transition in the antiferromagnetic material, Nat. Mater. **17**, 28 (2018).

[17] M. Weisheit, S. Fahler, A. Marty, Y. Souche, C. Poinsignon, and D. Givord, Electric field-induced modification of magnetism in thin-film ferromagnets, Science **315**, 349 (2007).

[18] C. Song, B. Cui, F. Li, X. Zhou, and F. Pan, Recent progress in voltage control of magnetism: Materials, mechanisms, and performance, Prog. Mater. Sci. **87**, 33 (2017).

[19] A. Molinari, H. Hahn, and R. Kruk, Voltage-Control of magnetism in all-solid-state and solid/liquid magnetoelectric composites, Adv. Mater. **31**, 1806662 (2019).

[20] C. Navarro-Senent, A. Quintana, E. Menéndez, E. Pellicer, and J. Sort, Electrolyte-Gated magnetoelectric actuation: Phenomenology, materials, mechanisms, and prospective applications, APL Mater. **7**, 030701 (2019).

[21] J. Zehner, I. Soldatov, S. Schneider, R. Heller, N. B. Khojasteh, S. Schiemenz, S. Fähler, K. Nielsch, R. Schäfer, and K. Leistner, Voltage-Controlled deblocking of magnetization reversal in thin films by tunable domain wall interactions and pinning sites, Adv. Electron. Mater. **6**, 2000406 (2020).

[22] M. Nichterwitz, S. Honnali, M. Kutuzau, S. Guo, J. Zehner, K. Nielsch, and K. Leistner, Advances in magnetoionic materials and perspectives for their application, APL Mater. **9**, 030903 (2021).

[23] Q. Yang, Z. Zhou, N. X. Sun, and M. Liu, Perspectives of voltage control for magnetic exchange bias in multiferroic heterostructures, Phys. Lett. A **381**, 1213 (2017).

[24] X. He, Y. Wang, N. Wu, A. N. Caruso, E. Vescovo, K. D. Belashchenko, P. A. Dowben, and C. Binek, Robust isothermal electric control of exchange bias at room temperature, Nat. Mater. **9**, 579 (2010).

[25] S. M. Wu, S. A. Cybart, D. Yi, J. M. Parker, R. Ramesh, and R. C. Dynes, Full Electric Control of Exchange Bias, Phys. Rev. Lett. **110**, 067202 (2013).

[26] P. Borisov, A. Hochstrat, X. Chen, W. Kleemann, and C. Binek, Magnetoelectric Switching of Exchange Bias, Phys. Rev. Lett. **94**, 117203 (2005).

[27] K. Toyoki, Y. Shiratsuchi, A. Kobane, C. Mitsumata, Y. Kotani, T. Nakamura, and R. Nakatani, Magnetoelectric switching of perpendicular exchange bias in Pt/Co/α-Cr 2 O 3 /Pt stacked films, Appl. Phys. Lett. **106**, 162404 (2015).

[28] U. Bauer, L. Yao, A. J. Tan, P. Agrawal, S. Emori, H. L. Tuller, S. van Dijken, and G. S. D. Beach, Magneto-Ionic control of interfacial magnetism, Nat. Mater. **14**, 174 (2015).

[29] A. J. Tan, M. Huang, C. O. Avci, F. Büttner, M. Mann, W. Hu, C. Mazzoli, S. Wilkins, H. L. Tuller, and G. S. D. Beach, Magneto-Ionic control of magnetism using a solid-state proton pump, Nat. Mater. **18**, 35 (2019).

[30] J. Grollier, D. Querlioz, K. Y. Camsari, K. Everschor-Sitte, S. Fukami, and M. D. Stiles, Neuromorphic spintronics, Nat. Electron. **3**, 360 (2020).

[31] J. Torrejon, M. Riou, F. A. Araujo, S. Tsunegi, G. Khalsa, D. Querlioz, P. Bortolotti, V. Cros, K. Yakushiji, A. Fukushima, H. Kubota, S. Yuasa, M. D. Stiles, and J. Grollier, Neuromorphic computing with nanoscale spintronic oscillators, Nature (London) **547**, 428 (2017).

[32] D. Ielmini and S. Ambrogio, Emerging neuromorphic devices, Nanotechnology **31**, 092001 (2020).

[33] Y. Li, Z. Wang, R. Midya, Q. Xia, and J. J. Yang, Review of memristor devices in neuromorphic computing: materials sciences and device challenges, J. Phys. Appl. Phys. **51**, 503002 (2018).

[34] J. Walter, B. Voigt, E. Day-Roberts, K. Heltemes, R. M. Fernandes, T. Birol, and C. Leighton, Voltage-Induced ferromagnetism in a diamagnet, Sci. Adv. **6**, eabb7721 (2020).

[35] V. K. Sangwan and M. C. Hersam, Neuromorphic nanoelectronic materials, Nat. Nanotechnol. **15**, 517 (2020).

[36] K. Leistner, J. Wunderwald, N. Lange, S. Oswald, M. Richter, H. Zhang, L. Schultz, and S. Fähler, Electric-Field control of magnetism by reversible surface reduction and oxidation reactions, Phys. Rev. B **87**, 224411 (2013).

[37] F. Maroun, F. Reikowski, N. Di, T. Wiegmann, J. Stettner, O. M. Magnussen, and P. Allongue, Potential dependence of the structure and magnetism of electrodeposited Pd/Co/Au(111) layers, J. Electroanal. Chem. **819**, 322 (2018).

[38] S. Robbennolt, E. Menéndez, A. Quintana, A. Gómez, S. Auffret, V. Baltz, E. Pellicer, and J. Sort, Reversible, electric-field induced magnetoionic control of magnetism in mesoporous cobalt ferrite thin films, Sci. Rep. **9**, 10804 (2019).

[39] U. Bauer, S. Emori, and G. S. D. Beach, Voltage-Controlled domain wall traps in ferromagnetic nanowires, Nat. Nanotechnol. **8**, 411 (2013).

[40] C. Bi, Y. Liu, T. Newhouse-Illige, M. Xu, M. Rosales, J. W. Freeland, O. Mryasov, S. Zhang, S. G. E. te Velthuis, and W. G. Wang, Reversible Control of Co Magnetism by Voltage-Induced Oxidation, Phys. Rev. Lett. **113**, 267202 (2014).

[41] L. Wei, Z. Hu, G. Du, Y. Yuan, J. Wang, H. Tu, B. You, S. Zhou, J. Qu, H. Liu, R. Zheng, Y. Hu, and J. Du, Full electric control of exchange bias at room temperature by resistive switching, Adv. Mater. **30**, 1801885 (2018).

[42] D. A. Gilbert, J. Olamit, R. K. Dumas, B. J. Kirby, A. J. Grutter, B. B. Maranville, E. Arenholz, J. A. Borchers, and K. Liu, Controllable positive exchange bias via redox-driven oxygen migration, Nat. Commun. **7**, 11050 (2016).

[43] J. Zehner, R. Huhnstock, S. Oswald, U. Wolff, I. Soldatov, A. Ehresmann, K. Nielsch, D. Holzinger, and K. Leistner, Nonvolatile electric control of exchange bias by a redox transformation of the ferromagnetic layer, Adv. Electron. Mater. **5**, 1900296 (2019).

[44] Q. Li, S. S. Yan, J. Xu, S. D. Li, G. X. Zhao, Y. Z. Long, T. T. Shen, K. Zhang, and J. Zhang, Electrical control of exchange bias via oxygen migration across CoO-ZnO nanocomposite barrier, Appl. Phys. Lett. **109**, 252406 (2016).

[45] Z. Mustafa, D. Pravarthana, B. Wang, H. Yang, and R.-W. Li, Manipulation of Exchange Bias Effect via All-Solid-State Li -Ion Redox Capacitor with Antiferromagnetic Electrode, Phys. Rev. Appl. **14**, 014062 (2020).

[46] X. Zhou, Y. Yan, M. Jiang, B. Cui, F. Pan, and C. Song, Role of oxygen ion migration in the electrical control of magnetism in Pt/Co/Ni/HfO_2 films, J. Phys. Chem. C **120**, 1633 (2016).

[47] A. J. Tan, M. Huang, S. Sheffels, F. Büttner, S. Kim, A. H. Hunt, I. Waluyo, H. L. Tuller, and G. S. D. Beach, Hydration of gadolinium oxide (Gd O_x) and its effect on voltage-induced Co oxidation in a Pt/Co/GdO_x/Au heterostructure, Phys. Rev. Mater. **3**, 064408 (2019).

[48] K.-Y. Lee, S. Jo, A. J. Tan, M. Huang, D. Choi, J. H. Park, H.-I. Ji, J.-W. Son, J. Chang, G. S. D. Beach, and S. Woo, Fast Magneto-Ionic Switching of Interface Anisotropy Using Yttria-Stabilized Zirconia Gate Oxide, Nano Lett. **20**, 3435 (2020).

[49] K. Klyukin, G. Beach, and B. Yildiz, Hydrogen tunes magnetic anisotropy by affecting local hybridization at the interface of

a ferromagnet with nonmagnetic metals, Phys. Rev. Mater. **4**, 104416 (2020).

[50] See Supplemental Material at http://link.aps.org/supplemental/10.1103/PhysRevMaterials.5.L061401 for more details on the influence of a large magnetic field on a virgin sample, a comparison between magnetization curves of a virgin area beneath the Au electrode and an area next to the virgin Au electrode as well as a discussion of the training and thermal after effect.

[51] F. Garcia, J. Sort, B. Rodmacq, S. Auffret, and B. Dieny, Large anomalous enhancement of perpendicular exchange bias by introduction of a nonmagnetic spacer between the ferromagnetic and antiferromagnetic layers, Appl. Phys. Lett. **83**, 3537 (2003).

[52] M. Liu, J. Lou, S. Li, and N. X. Sun, E-Field control of exchange bias and deterministic magnetization switching in AFM/FM/FE multiferroic heterostructures, Adv. Funct. Mater. **21**, 2593 (2011).

[53] A. Mougin, T. Mewes, M. Jung, D. Engel, A. Ehresmann, H. Schmoranzer, J. Fassbender, and B. Hillebrands, Local manipulation and reversal of the exchange bias field by ion irradiation in FeNi/FeMn double layers, Phys. Rev. B **63**, 060409(R) (2001).

[54] T. Ueltzhöffer, C. Schmidt, I. Krug, F. Nickel, D. Gottlob, and A. Ehresmann, Néel walls between tailored parallel-stripe domains in IrMn/CoFe exchange bias layers, J. Appl. Phys. **117**, 123904 (2015).

[55] K. Liu, S. M. Baker, M. Tuominen, T. P. Russell, and I. K. Schuller, Tailoring exchange bias with magnetic nanostructures, Phys. Rev. B **63**, 060403(R) (2001).

[56] E. Albisetti, D. Petti, M. Pancaldi, M. Madami, S. Tacchi, J. Curtis, W. P. King, A. Papp, G. Csaba, W. Porod, P. Vavassori, E. Riedo, and R. Bertacco, Nanopatterning reconfigurable magnetic landscapes via thermally assisted scanning probe lithography, Nat. Nanotechnol. **11**, 545 (2016).

[57] Y. J. Tang, B. Roos, T. Mewes, S. O. Demokritov, B. Hillebrands, and Y. J. Wang, Enhanced coercivity of exchange-bias Fe/MnPd bilayers, Appl. Phys. Lett. **75**, 707 (1999).

[58] J. M. Barandiarán, J. Gutiérrez, and A. García-Arribas, Magneto-Elasticity in amorphous ferromagnets: Basic principles and applications, Phys. Status Solidi A **208**, 2258 (2011).

[59] D. Atkinson, P. T. Squire, M. R. J. Gibbs, and S. N. Hogsdon, Implications of magnetic and magnetoelastic measurements for the domain structure of FeSiB amorphous wires, J. Phys. Appl. Phys. **27**, 1354 (1994).

[60] M. Han, D. F. Liang, and L. J. Deng, Sensors development using its unusual properties of Fe/Co-Based amorphous soft magnetic wire, J. Mater. Sci. **40**, 5573 (2005).

[61] L. Xia, K. C. Chan, L. Zhao, D. Ding, and B. Z. Tang, Magnetic properties and magnetostriction of a binary Dy_{50}/Co_{50} amorphous alloy, J. Non-Cryst. Solids **493**, 29 (2018).

[62] N. Eliaz and D. Eliezer, An overview of hydrogen interaction with amorphous alloys, Adv. Perform. Mater. **6**, 5 (1999).

[63] R. C. Bowman Jr., Preparation and properties of amorphous hydrides, Mater. Sci. Forum **31**, 197 (1988).

[64] A. Hubert and R. Schäfer, *Magnetic Domains* (Springer, Berlin, 1998).

[65] R. Hilzinger and W. Rodewald, *Magnetic Materials: Fundamentals, Products, Properties, and Applications* (VACUUMSCHMELZE, Hanau, Germany, 2013).

[66] W. Echtenkamp and C. Binek, Electric Control of Exchange Bias Training, Phys. Rev. Lett. **111**, 187204 (2013).